# SUPPORTING INFORMATION

## Table of Contents

**S1.   Experimental**

*Synthesis of Nanoparticles of Amorphous Calcium Carbonate (ACC)*

2 L ethanol (99.9%, VWR No. 20820.293) were stirred in a 2 L plastic beaker (PP).

50 mL of 10 mM calcium chloride solution (prepared from calcium chloride

hexahydrate, Sigma-Aldrich No. 21108) were added, and after stirring for 2 min, 50

mL of 10 mM sodium carbonate solution (prepared from sodium carbonate, Sigma-

Aldrich No. S7795) was added. Then, the beaker was sealed with Parafilm and after

stirring for ca. 30 min, the magnetic stirrer was removed, the beaker re-sealed, and

left standing for ca. 30 min. The supernatant was carefully decanted, and the

remaining, slightly opaque sediment of ACC was centrifuged at ~6000 $g$

(gravitational acceleration $g$ = 9.81 m·s$^{-2}$). The sediment was washed in 50 mL pure

ethanol, followed by 50 mL pure acetone (VWR No. 20066.296), and eventually dried

in vacuo. The yield is ca. 50 mg of ACC per synthesis.

*Preparation of Nanocrystalline Cellulose (NCC)*

The suspension of nanocrystalline cellulose (NCC) was prepared from

microcrystalline cellulose (Avicel PH200) by sulfuric acid hydrolysis.[1] In brief, 20 g of

cellulose was stirred with 175 mL of 64 *wt*% sulfuric acid at 45 °C for 40 min. The

suspension was diluted 10-fold with deionized water and then centrifuged at 4500

rpm for 20 min to concentrate the cellulose and to remove excess aqueous acid. The

resultant precipitate was rinsed, centrifuged, and dialyzed against deionized water for

7 days until constant neutral pH was achieved. The suspension was sonicated 2×5

min (Branson Sonifier Model 250 ultrasonic cell disruptor/homogenizer) at 80 %

output (with cooling in an ice bath) to create cellulose crystals of colloidal

dimensions. Mixed bed ion-exchange resin (Dowex Marathon MR-3 hydrogen and

hydroxide form) was added to the cellulose suspension for 48 h and then removed by filtration. Dry content of the suspensions were determined by gravimetry.

*Determination of NCC Sulfonate Content*

The sulfonate content of NCC was determined by conductometric titration. Typically, 50 mg of NCC were suspended in 50 mL of deionized water containing 1 mM NaCl. The titration was performed using 0.0114 M NaOH solution standardized against oxalic acid and measured with a conductometer (Mettler Toledo). A sulfonate content of 0.34 mmol·g$^{-1}$ was thus evaluated.

*Preparation of Coatings*

Coatings were prepared from ethanol-based dispersions as follows: 1 mL of the dispersions described above was added to 50 mL ethanol in a 50 mL centrifuge tube with conical bottom, thoroughly shaken, and sonicated for 2 min in an ultrasonic bath. A silicon wafer or a quartz substrate (~1 × 1 cm$^2$) was placed at the bottom of the centrifuge tube, and the tube was placed in a Hettich EBA 21 centrifuge equipped with an angle rotor (No. 1116): special care was taken that the surface of the wafer was aligned perpendicular to the centrifugal field. The dispersions were centrifuged for 10 min at ~6000 *g*. After centrifugation, the wafers were completely covered by a transparent, albeit slightly opaque layer, which was ca. 0.5 mm thick. The coatings were then slowly dried in a vessel nearly saturated with ethanol, and had a single hole of ~4 mm diameter. The coatings were removed after ca. 36 h of drying and stored in a dessicator.

*Thermogravimetric Analysis (TGA)*

TGA was performed on a Perkin Elmer Thermogravimetric Analyzer TGA7. About 5 mg of the different hybrids (dried in vacuo from the dispersions in acetone for ~12 h) were analyzed under technical air (79 % $N_2$, 21 % $O_2$) from 50 ºC to 900 ºC at a heating rate of 2 ºC·min$^{-1}$.

*Scanning Electron Microscopy (SEM)*

SEM was measured on a JEOL JSM-7401F microscope in secondary electron imaging mode at an acceleration voltage of 2 kV. Coatings of the hybrids deposited on silicon wafers were glued to aluminium stubs using carbon-ink. Only where indicated, samples were coated with a thin carbon layer.

*X-ray Powder Diffraction (XRD)*

XRD patterns of fine-ground powder samples were recorded using $CuK_{\alpha 1}$ radiation and a PANalytical Xpert PRO MPD diffractometer equipped with a PIXcel detector at room temperature. Diffractograms were acquired in between 20º < 2θ < 60º at a scanning speed of 0.04 º·s$^{-1}$.

*Small Angle X-ray Scattering (SAXS)*

SAXS curves of a neat powder of ACC nanoparticles spread on Kapton were recorded at room temperature at the beamline i711 at MAX-lab (Lund, Sweden).[2,3] The observed 2D patterns were corrected for empty-beam scattering (Kapton), and transformed into a 1D radial averages of the scattering intensity using the Fit2D software (calibration with silver behenate).[4] The SAXS curves were evaluated utilizing the program SCATTER.[5]

*Atomic Force Microscopy (AFM)*

AFM topography micrographs were recorded in tapping mode in air with the aid of a MultiMode instrument with NanoScope V controller (Veeco, Santa Barbara, CA, USA). MPP-11100-10 silicon AFM probes (Veeco) with nominal spring constants of 40 N/m were used. The force was kept minimal during scanning by routinely decreasing it until the tip left the surface and subsequently increasing it slightly to just regain contact. The scan rate was 0.5 to 2 lines per second. All images with 512×512 pixels were analyzed with non-commercial software WSxM© (Nanotec Electronica, http://www.nanotec.es).

*Transmission Electron Microscopy (TEM)*

A drop of a diluted aqueous suspension of NCC (~0.1 *wt*%) was deposited on a bacitracin pre-treated surface of a TEM carbon coated copper grid to improve the dispersion of the NCC on the grid. The specimens were observed using a Philips Tecnai 10 electron microscope operated at 80 kV.

*UV-Visible spectrophotometry (UVVis)*

The visible on-line transmittance spectra of NCC-ACC hybrid films spin-coated on quartz (film thickness ~ 10 μm) were acquired with a Perkin-Elmer Lambda 19 UV/VIS/NIR spectrophotometer.

*Mechanical Properties*

The mechanical properties (hardness and reduced elastic modulus) were evaluated using an Ultra-Micro-Indenter system equipped with a Berkovich pyramidal-shaped diamond tip. The value of maximum applied force was chosen to be 100 mN to ensure that the maximum penetration depth during the tests was kept below one tenth of the overall film thickness (a necessary condition to avoid having an influence of the substrate on the measured mechanical properties of the film). The thermal drift during nanoindentation was kept below 0.05 nm·s$^{-1}$. Proper corrections for the contact area (calibrated with a fused quartz specimen), instrument compliance, and initial penetration depth were applied. The hardness ($H$) and reduced elastic modulus ($E_r$) values were derived from the load-displacement curves at the beginning of the unloading segment using the method of Oliver and Pharr.[6] From the initial unloading slope, the contact stiffness, $S$, was determined as:

$$S = \frac{dP}{dh}$$

where $P$ and $h$ denote, respectively, the applied load and the penetration depth during nanoindentation. The elastic modulus was evaluated based on its relationship with the contact area, $A$, and contact stiffness:

$$S = \beta \frac{2}{\sqrt{\pi}} E_r \sqrt{A}$$

Here, $\beta$ is a constant that depends on the geometry of the indenter ($\beta$ = 1.034 for a Berkovich indenter), and $E_r$ is the so-called reduced Young's modulus, defined as follows[7]:

$$\frac{1}{E_r} = \frac{1-v^2}{E} + \frac{1-v_i^2}{E_i}$$

The reduced modulus takes into account the elastic displacements that occur in both the specimen, with Young's modulus $E$ and Poisson's ratio $v$, and the diamond indenter, with elastic constants $E_i$ and $v_i$. Note that for diamond, $E_i$ = 1140 GPa and $v_i$ = 0.07. Remarkably, for most materials, including NCC or ACC, where $v \sim 0.3$ and 0.35, respectively (see Refs. 8 and 9), the contribution of the tip to $E_r$ is almost negligible, i.e., $E_r \approx E$. Hardness was calculated from the following expression:

$$H = \frac{P_{Max}}{A}$$

where $P_{Max}$ is the maximum load applied during nanoindentation. It should be noted that the ratio between hardness and reduced elastic modulus ratio, $H/E_r$, is recognized to provide a reliable assessment of the wear resistance behaviour of the film.[10]

Finally, the elastic recovery was evaluated as the ratio between the elastic and the total (plastic + elastic) energies during nanoindentation, $W_{el}/W_{tot}$. These energies were calculated from the nanoindentation experiments as the areas between the unloading curve and the x-axis ($W_{el}$) and between the loading curve and x-axis ($W_{tot}$).[7] The results presented here represent the statistical average of a set of 50 indentations for each sample.

**S2.  Figures**

A

B

Intensity (arbitrary unit)

ACC
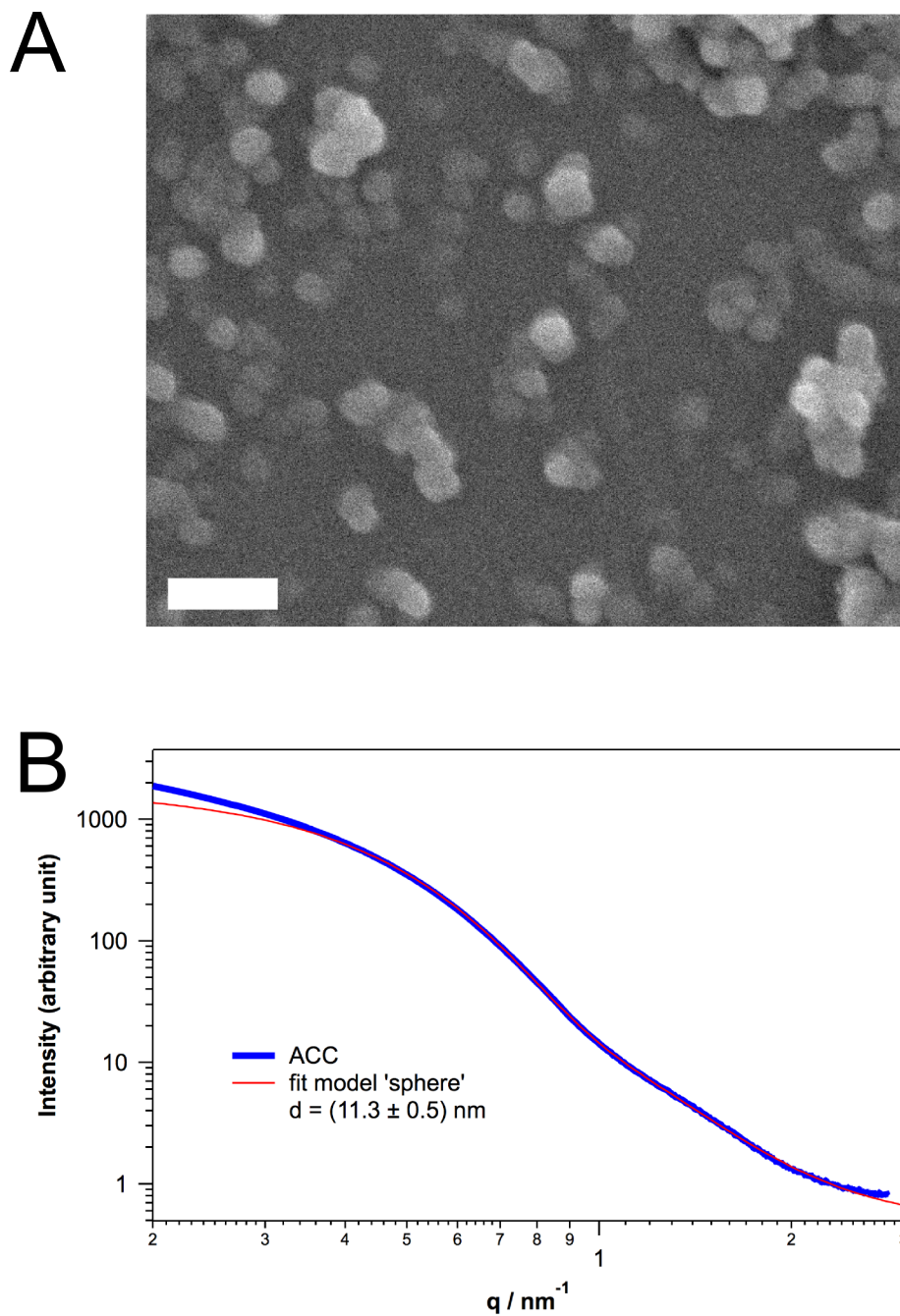fit model 'sphere'
d = (11.3 ± 0.5) nm

$q\ /\ nm^{-1}$

**Figure S1.** (a) SEM micrograph of carbon-coated ACC nanoparticles. The carbon coating is typically ~10 nm thick. Scale bar: 100 nm. (b) SAXS curve of a dry powder of neat ACC nanoparticles (blue trace). Fit of the SAXS curve gives the diameter of the spherical nanoparticles (red trace).
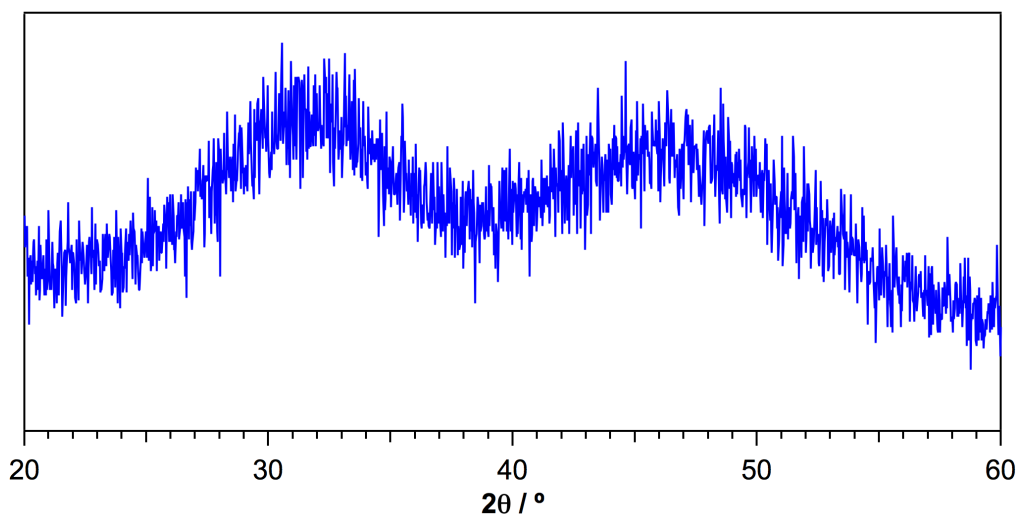
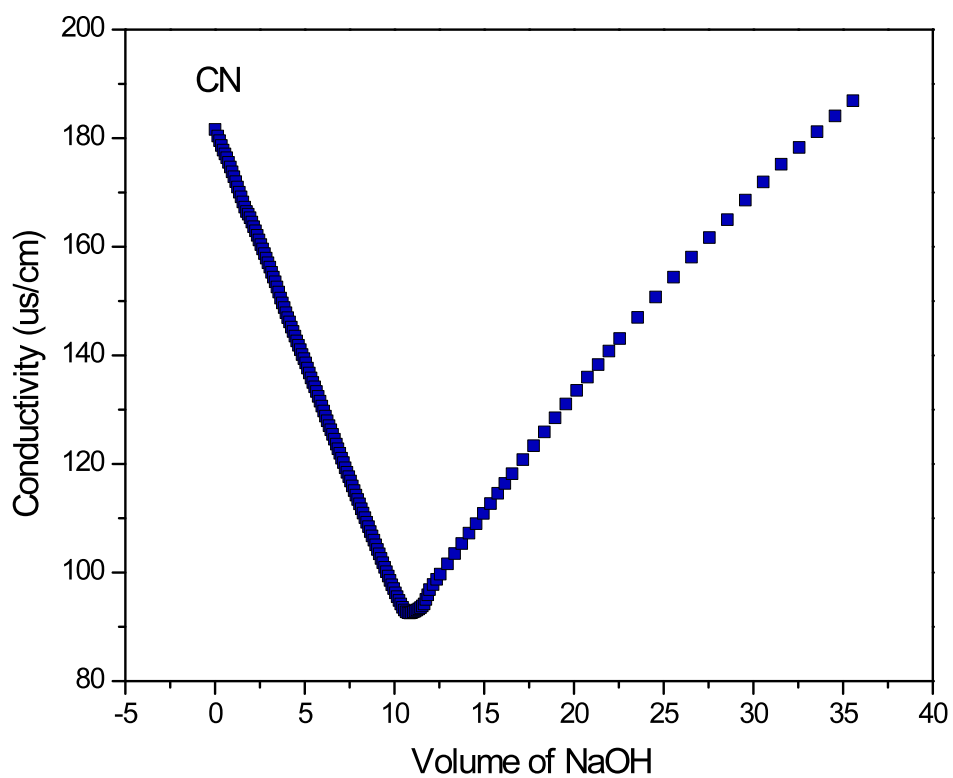**Figure S2.** WAXS curve of ACC nanoparticles demonstrating their amorphous character.



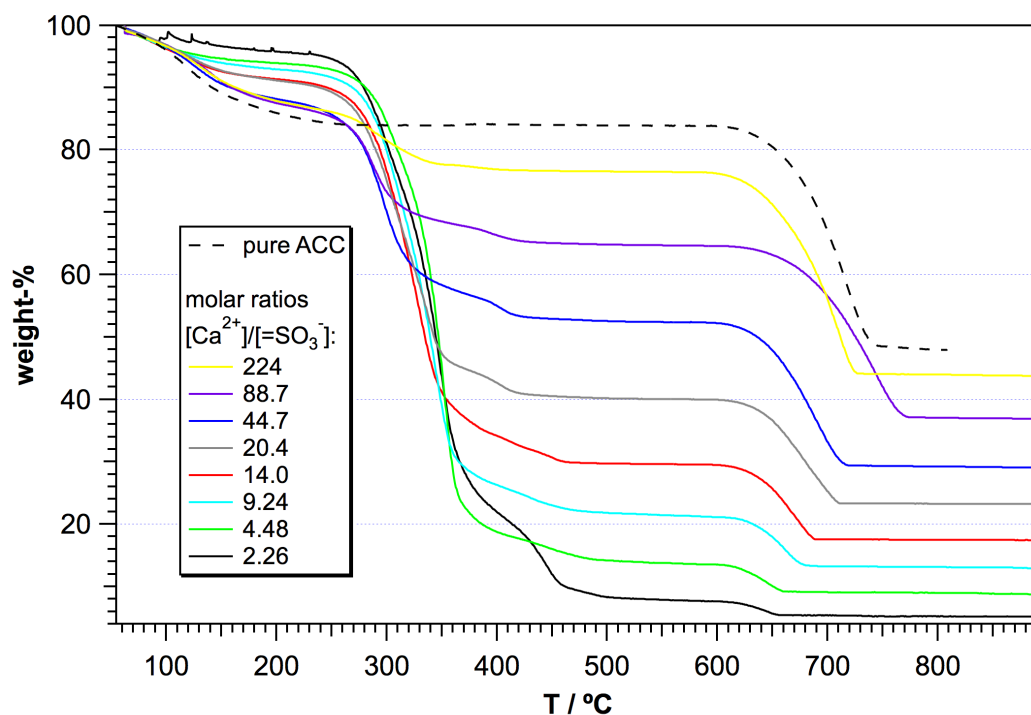**Figure S3.** Conductimetric titration of NCC with NaOH.

**Figure S4.** Thermogravimetric analyses of the pure ACC (note it is stoichiometric $CaCO_3 \cdot H_2O$) and of the different hybrids synthesized from a broad range of molar ratios $[Ca^{2+}]/[SO_3^-]$ (see Table S1). The first weight loss between ~60 °C and 250 °C corresponds to the release of (structural) water. The second weight loss from ~280 – 500 °C is due to the removal of NCC. Finally, weight loss starting at ~600 – 650 °C corresponds to the calcination of calcium carbonate into calcium oxide and gaseous carbon dioxide.
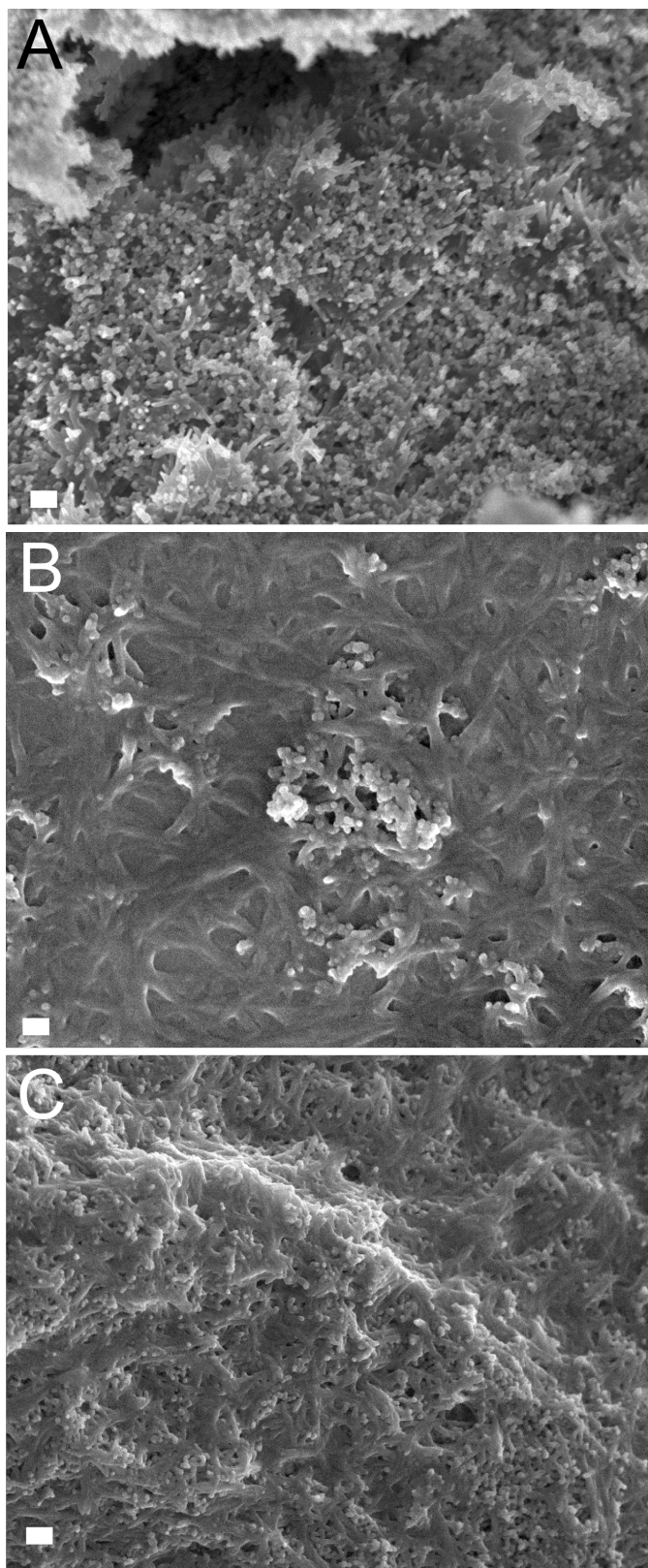
**Figure S5.** Microscopy images of hybrids with different compositions. Note that the samples were coated with a ~10 nm thick layer of carbon for SEM. (a) most homogeneous hybrid with ~30% ACC, (b) NCC with ~14% ACC, and (c) ~53% ACC. Scale bars: 100 nm.
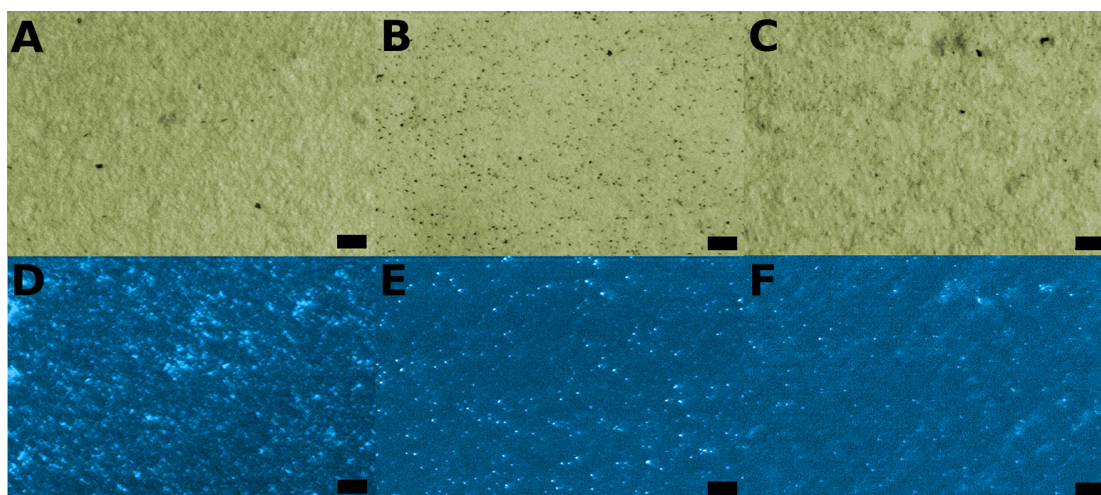
**Figure S6.** Optical microscopy images of coatings of NCC-ACC hybrids with different compositions on quartz (~1 × 1 cm$^2$) under normal illumination (top row) and cross-polars (bottom row). (a, d) NCC with ~14 *wt*% ACC, (b, e) most homogeneous hybrid with ~30 *wt*% ACC, and (c, f) ~53 *wt*% ACC. Scale bar corresponds to 50 μm. The size of the NCC ordered domains (bright regions in d-f) decreases as the ACC content increases.



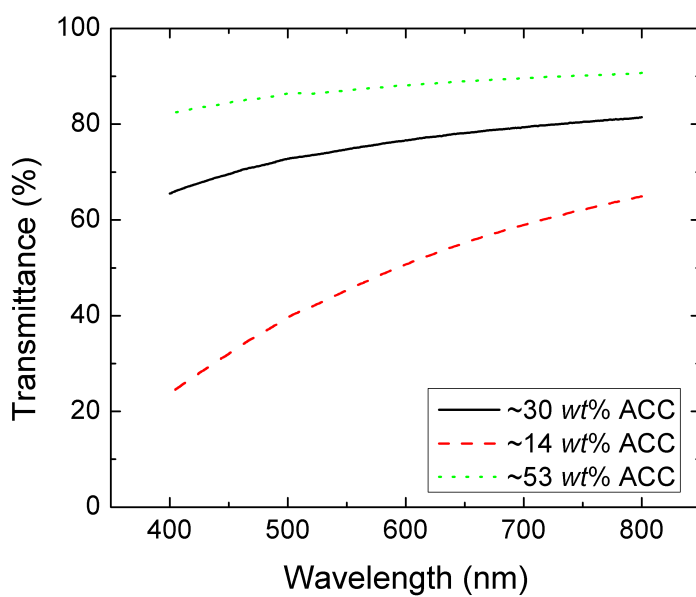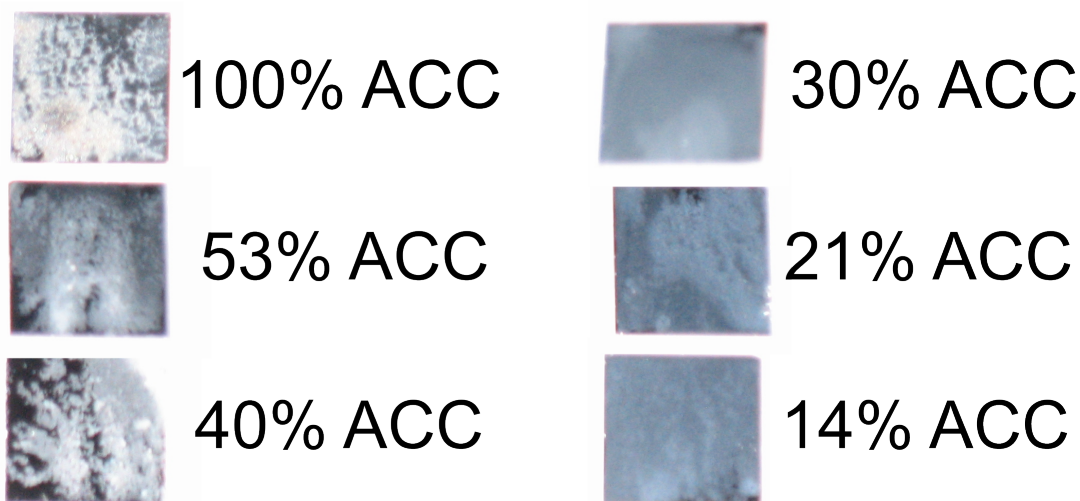**Figure S7.** Visible on-line transmittance spectra of coatings of NCC-ACC hybrids with different compositions on quartz (~1 × 1 cm$^2$).

**Figure S8.** Photographs of coatings of NCC-ACC hybrids with different compositions on silicon wafers (~1 × 1 cm$^2$) as indicated. The hybrid with ~30 $wt$% ACC forms the most continuous coating after drying. Wet coatings were continuous in all cases before drying.
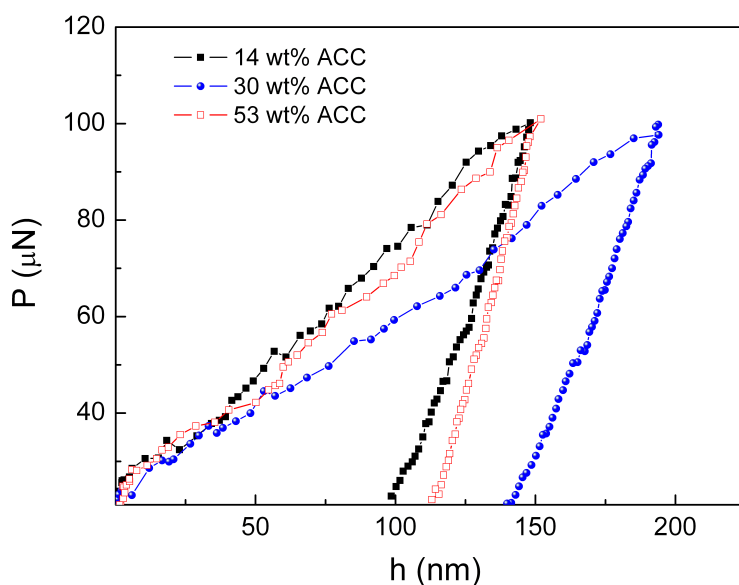


**Figure S9.** Representative load ($P$) – displacement ($h$) nanoindentation curves corresponding to hybrid films with 14 $wt$%, 30 $wt$% and 53 $wt$% ACC, measured to a $P_{max}$=100 mN. Note that the penetration depth in the hybrid film with 30 $wt$% is larger than for the other two samples, indicating that this film is the mechanically softest one. In turn, the contact stiffness (i.e., the slope of the unloading indentation segment) in the sample with 53 $wt$% ACC is more pronounced than for the other two films, suggesting a larger Young's modulus for this composition (see Table 1).

## S3. Tables

**Table S1.** Details for the synthesis of the NCC/ACC hybrids: Volumes of solutions, and NCC precursor concentrations, employed for the syntheses of the different ACC/NCC hybrids, and the concentrations of the different dispersion in acetone. The rightmost column gives the weight-% of ACC in the dry hybrid as determined by TGA.

| $Ca^{2+}$/SO3H ratio [mol/mol] | concentration NCC solution [mg/mL] | volume NCC solution [mL] | volume $Ca^{2+}$ solution [mL] | volume $CO_3^{2-}$ solution [mL] | concentration of dispersion [mg/mL] | Nominal weight-% ACC in hybrid | Exp. weight-% ACC in hybrid |
|---|---|---|---|---|---|---|---|
| 2.26 | 13.0 | 10 | 10 | 10 | 5 | 7 | 8 |
| 4.48 | 19.9 | 3.3 | 10 | 10 | 3 | 13 | 14 |
| 9.24 | 19.9 | 1.6 | 10 | 10 | 5 | 24 | 21 |
| 14.0 | 19.9 | 10.5 | 100 | 100 | 23 | 32 | 30 |
| 20.4 | 13.0 | 10 | 90 | 90 | 47 | 41 | 40 |
| 44.7 | 19.9 | 1.6 | 48.4 | 48.4 | 16 | 60 | 53 |
| 88.7 | 19.9 | 0.8 | 49.2 | 49.2 | 9 | 75 | 65 |
| 224 | 13.0 | 1 | 99 | 99 | 44 | 88 | 76 |

**Table S2.** Additional mechanical properties of the hybrid ACC/NCC films obtained from nanoindentation experiments. Parentheses indicate the standard deviation in the last digits.

| wt% ACC | Wear resistance $H/E_r$ | Plastic energy $W_p$ (nJ) | Elastic energy $W_{el}$ (nJ) | Total indentation energy $W_{tot}$ (nJ) | Elastic recovery $W_{el}/W_{tot}$ |
|---|---|---|---|---|---|
| 14 | 0.116(9) | 0.0062(2) | 0.0040(1) | 0.0102(2) | 0.392(12) |
| 30 | 0.089(10) | 0.0089(2) | 0.0035(1) | 0.0124(2) | 0.282(9) |
| 53 | 0.064(4) | 0.0063(3) | 0.0024(1) | 0.0087(3) | 0.278(14) |

## S4.  References

1.  Cranston, E.D. & Gray, D.G. Morphological and Optical Characterization of Polyelectrolyte Multilayers Incorporating Nanocrystalline Cellulose. *Biomacromolecules* **7**, 2522-2530 (2006).

2.  Cerenius, Y. et al. The crystallography beamline I711 at MAX II. *J. Synchrotron Rad.* **7**, 203-208 (2000).

3.  Knaapila, M. et al. A new small-angle X-ray scattering set-up on the crystallography beamline I711 at MAX-lab. *J. Synchrotron Rad.* **16**, 498-504 (2009).

4.  Hammersly, A. THE FIT2D HOME PAGE. at <http://www.esrf.eu/computing/scientific/FIT2D/>

5.  Förster, S. FB Chemie : Institute und Abteilungen : Physikalische Chemie : Arbeitskreis S. Förster : Software. at <http://www.chemie.uni-hamburg.de/pc/sfoerster/software.html>

6.  Oliver, W.C., Pharr, G. M. *J. Mater. Res.* **7,** 1564-1583 (1992).

7.  Fischer-Cripps, A. C. in Nanoindentation (Ed: F. F. Ling), Springer, New York 2004.

8.  Prokhorova, D.A., Chatterjee, A.P. *Biomacromolecules* **10**, 3259–3265 (2009).

9.  Faatz, M., Cheng, W., Wegner, G. *Langmuir* **21**, 6666–6668 (2005).

10. Leyland, A., Matthews, A. *Wear* **246**, 1-11 (2000).